Ferromagnetism of Pt nanoparticles induced by surface chemisorption

Yasuhiro Sakamoto, Yojiro Oba, Hideyuki Maki, Masayuki Suda, Yasuaki Einaga, and Tetsuya Sato
School of Integrated Design Engineering, Graduate School of Science and Technology, Keio University, 3-14-1 Hiyoshi, Kohoku-ku, Yokohama, Kanagawa 223-8522, Japan

Masaichiro Mizumaki, Naomi Kawamura, and Motohiro Suzuki
Japan Synchrotron Radiation Research Institute (JASRI/SPring-8), 1-1-1, Kouto, Sayo-cho, Sayo-gun, Hyogo 679-5198, Japan
(Received 23 March 2010; revised manuscript received 4 February 2011; published 28 March 2011)

The magnetic properties of different-sized Pt nanoparticles coated by alkanethiol molecules with different carbon chain lengths (1-octadecanethiol, 1-dodecanthiol, and 1-octanethiol) were systematically studied by means of magnetic measurement, x-ray magnetic circular dichroism (XMCD), x-ray absorption near-edge structure (XANES), and electron spin resonance (ESR). Furthermore, azobenzene-derivatized thiol coating of Pt nanoparticles was performed to detect the effect on magnetic characteristics of the geometrical transformation between *cis* and *trans* states induced by photoisomerization. All samples showed the ferromagnetism inherent in Pt. In all of the prepared particles Curie temperatures above 300 K were observed. The largest magnetization at 5 K was observed for the longest chain length of alkanethiol and the smallest particle size. The coercive force at 5 K increased as the chain length increased and the particle size decreased. The geometrical transformation of coated molecules barely affected the magnetization and coercive force. The increase in coercive force was accompanied by the enhanced contribution of the orbital magnetic moment. The origins of ferromagnetism and magnetic anisotropy in Pt nanoparticles are discussed in terms of the contribution from the coating molecules and downsizing effects. The appearance of ferromagnetism is mainly interpreted based on two mechanisms, i.e., the electronic band magnetism based on the Stoner criterion for ferromagnetism and the orbital ferromagnetism due to electrons captured in the atomiclike orbital on the particle surface. The chain-length and particle-size-dependent magnetic anisotropy is explained in terms of the change in angular momentum depending on the adsorption condition, especially the coverage ratio, of alkanethiol on the particle surface. This is consistent with the existence of orbital ferromagnetism in the Pt nanoparticle.

DOI: 10.1103/PhysRevB.83.104420 PACS number(s): 75.75.Lf, 75.30.Gw

I. INTRODUCTION

Nanoparticles have been studied intensively because of their potential in practical applications, such as high-density storage media, catalysts, and electronic devices, and because of their fundamental properties.[1–4] On the nanometer scale, the change in electronic states due to the reduced size brings about exotic physical properties which are quite different from those of bulk materials. For example, the appearance of ferromagnetism in nanoparticles of nonmagnetic metals such as the late transition metals (Pd and Pt) and gold has been extensively reported.[5–11] These researches have presented a new dimension in nanophysics and have created new opportunities in the development of magnetic materials, although a comprehensive interpretation of the phenomena is still anticipated.

The magnetism of exchange-enhanced magnetic materials, e.g., Pd and Pt, has been characterized based on the peculiar band structure in which the density of states at Fermi energy $D(E_F)$ almost satisfies the Stoner criterion for ferromagnetism $I\,D(E_F) > 1$, where I is a Stoner exchange integral.[12–14] Thus, the change in the electronic structure that takes place in the nanodimension can cause a pronounced change in magnetism. From this viewpoint, experimental and theoretical studies of ferromagnetism in nanosized systems of Pd have been intensively performed.[5,6,15–22] In addition, theoretical studies of the magnetic nature of Pt thin films[15,16] and nanowires[23] have predicted the appearance of ferromagnetism in certain structures. Recently, the ferromagnetic behavior of Pt nanoparticles prepared using a chemical method was reported.[8,9] In these reports, the origin of ferromagnetism was attributed to the change in structure symmetry due to twin formation or surface effects and the charge transfer from the molecules coating the nanoparticle. On the other hand, large magnetic anisotropy due to strong spin-orbit interaction is predicted for Pt nanowires. Thus, the magnetic anisotropy is widely tunable in nanosized systems of Pt through the change in electronic structure[24] and the modification of surface conditions such as the surface chemisorption,[25] although there has been no detailed experimental information on magnetic anisotropy in ferromagnetic Pt. This makes nanosized Pt systems attractive for basic investigations as well as for practical applications, e.g., in data storage. Therefore, it is worthwhile to clarify the nature of the magnetic anisotropy of ferromagnetic Pt in nanosized systems and to discover how to manipulate the magnetic anisotropy based on size and material parameters.

In the present paper, we demonstrate the appearance of ferromagnetism in Pt nanoparticles of different particle sizes and coated by alkanethiols of various carbon chain lengths, by means of magnetic measurement and x-ray magnetic circular dichroism (XMCD). The magnetic anisotropy, which is dependent on the chain length of coating molecules and particle size, is evaluated based on coercive force and electron spin resonance (ESR). In addition, the magnetic properties of the Pt nanoparticles coated by azobenzene-derivatized thiols in *trans* and *cis* states, which can be changed through photoisomerization, are studied to clarify the contribution

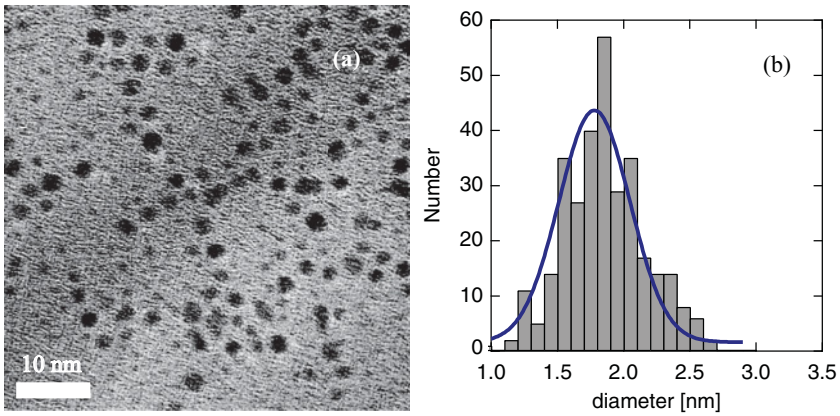

FIG. 1. TEM image (a) and size distribution histogram (b) of ODT-Pt1 with $d = 1.9$ nm.

of the molecule geometry to the magnetic anisotropy of the interior nanoparticle. The tunable magnetic anisotropy is discussed in terms of the orbital angular momentum in relation to two mechanisms: the change in the hole concentration in the 5*d* band of Pt induced by the charge transfer from the coating molecules and the modification of band structure, and the surface structure of molecules adsorbed on the Pt nanoparticle.

II. EXPERIMENTAL

The Pt nanoparticles to be coated with an alkanethiol were prepared by two different methods (methods I and II).

Method I: The synthesis of Pt nanoparticles followed the procedure of a previous report.[26] Dihydrogen hexachloroplatinate (IV) hexahydrate (0.5 mmol) and alkanethiol (AT) (0.5 mmol) were dissolved in 10 mL of tetrahidrofuran (THF), and then a solution of lithium triethylborohydride in THF (1.0 M, 10 mL) was added. After stirring for 40 min, colloidal Pt nanoparticles were formed. The nanoparticles were precipitated by the addition of ethanol to the reacted solution, followed by centrifugation. Ethanol was added again to the precipitate and centrifugal separation was performed again. This process was repeated several times; then the nanoparticles were dried. Using this synthesis process, 1-octadecanethiol (ODT), 1-dodecanthiol (DT), and 1-octanethiol (OT) coated Pt nanoparticles with ∼2 nm in diameter *d* were prepared, with methanol used to precipitate the DT- and OT-coated Pt nanoparticles instead of ethanol.

Method II: This synthesis process is based on the hot soap method.[9,27] First, platinum (II) acetylacetonate (0.25 mmol) was dissolved in oleylamine (3 mL) at 70 °C by stirring it in an Ar atmosphere for 12 h. Then the solution was injected into 10-mL oleylamine at 250 °C and stirred for 1 h. The black solution was cooled to room temperature by removal of the heat source. Methanol (20 mL) was added to the reaction medium, and samples were precipitated by centrifugation (3500 rpm, 10 min). Methanol was added again to the precipitate, and centrifugal separation was performed again. This process was repeated several times; then the nanoparticles were dried. Using this synthesis process, ODT-coated Pt nanoparticles with $d = 5.6$ and 7.3 nm were prepared.

For the coating of Pt nanoparticles by azobenzene-derivatized thiols, azobenzene-derivatized ligands, 4-(4-phenylazo-phenoxy)-butane-1-thiol (AZO), were obtained from [4-(4-bromo-butoxy)-phenyl]-phenyl-diazene, which had been synthesized earlier.[28,29] AZO-coated Pt nanoparticles with diameters of 1.3 and 6.5 nm were prepared based on methods I and II, respectively, with AZO used instead of alkanethiol in the synthesis processes.

A transmission electron microscope (TEM) image of OCT-Pt1 ($d = 1.9$ nm) and a size distribution histogram of synthesized particles are shown in Fig. 1. The nanoparticles have a spherical shape and diameter according to Gaussian size distribution. The sample sizes of OT-Pt, DT-Pt, and ODT-Pt1 were intrinsically the same. Figure 2 compares the particle size distributions of ODT-Pt1, ODT-Pt2, and ODT-Pt3, where the distribution increases with increasing particle size. A composition analysis using inductively coupled plasma atomic emission spectroscopy (ICP-AES) showed that the typical content of the ferromagnetic Fe impurity was less than 13 ppm. The characteristics of prepared Pt nanoparticles including AZO-coated Pt nanoparticles are summarized in Table I.

Magnetic measurements were performed by a superconducting quantum interference device (SQUID) magnetometer below 300 K. When the magnetization of AZO-coated Pt nanoparticles was measured, a quartz waveguide 50 nm in diameter was inserted into the SQUID magnetometer to illuminate the samples with ultraviolet (UV) or visible light.

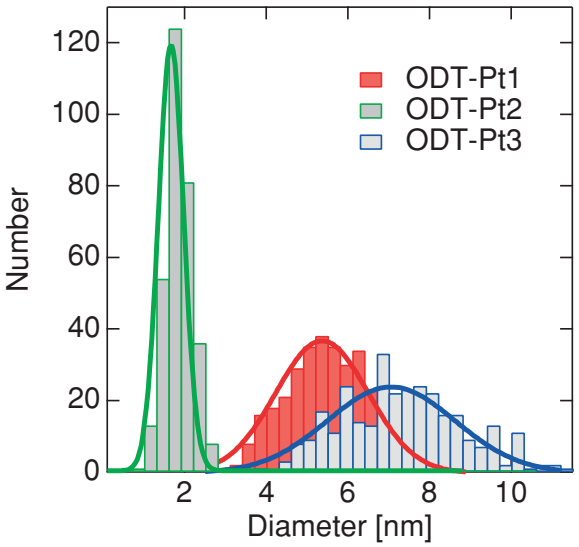

FIG. 2. (Color online) Particle size distributions of ODT-Pt1, ODT-Pt2, and ODT-Pt3.

TABLE I. Prepared nanoparticle samples, used surfactant, preparation conditions, and average diameters.

Sample	Surfactant	Preparation method	Average diameter (nm)
OT-Pt	1-octanehiol (OT)	1	2.2
DT-Pt	1-dodecanethiol (DT)	1	2.0
ODT-Pt1	1-octadecanethiol (ODT)	1	1.9
ODT-Pt2	1-octadecanethiol (ODT)	2	5.6
ODT-Pt3	1-octadecanethiol (ODT)	2	7.3
AZO-Pt	4-(4-phenylazo-phenoxy)-butane-1-thiol (AZO)	1	1.3
AZO-Pt2	4-(4-phenylazo-phenoxy)-butane-1-thiol (AZO)	2	6.5

The ESR spectra were obtained at room temperature using an x-band spectrometer.

The XMCD experiments were performed at the beamline BL39XU of SPring-8.[30] The spectra of the x-ray absorption near-edge structure (XANES) and XMCD were obtained in the transmission mode. Circularly polarized x rays were obtained using a diamond quarter-wave plate.[31] The XMCD spectra were measured by the helicity reversal method using an electromagnet in a magnetic field of 6 kOe at ~30 K, with the magnetic field applied parallel to the direction of the incident x rays. The incident photon energies of ~11.6 and ~13.3 keV were used for measurements around the L_3 and L_2 edges of Pt, respectively.

Optical absorption spectra of AZO were obtained using a conventional UV-visible spectrometer to detect the reversible photoisomerization under illumination by UV and visible light (Fig. 3). After illumination by UV light, an increase and decrease in peak intensities were observed at ~440 and ~350 nm, corresponding to the *cis* and *trans* states, respectively. Furthermore, the spectrum intrinsically recovered to the initial profile after illumination by visible light. Thus, reversible photoisomerization occurred in the present AZO-coated particles.

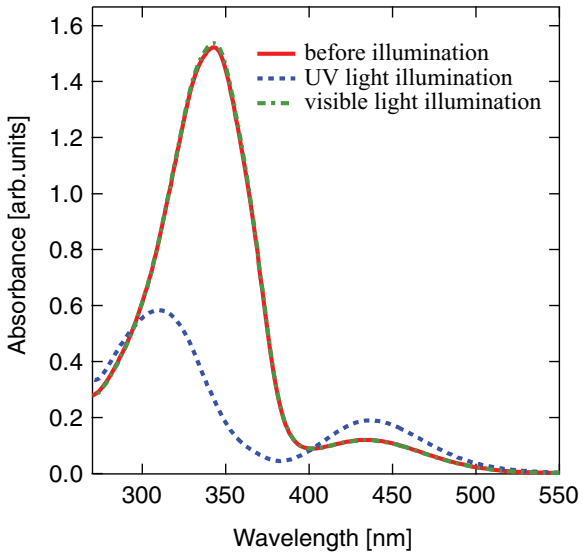

FIG. 3. (Color online) Optical absorption spectra of 4-(4-phenylazo-phenoxy)-butane-1-thiol (AZO) under illumination of UV and visible light.

III. EXPERIMENTAL RESULTS

A. Ferromagnetic behavior of ODT-Pt1

The magnetization curves of ODT-Pt1 at various temperatures in Fig. 4(a) show saturation behavior in magnetic fields higher than ~2 kOe at temperatures below 300 K and hysteresis behavior at low temperatures, where the magnetization of nanoparticles is obtained by subtracting the magnetic contributions from the sample holder and alkenethiol molecules under the assumption that they are linearly dependent on the magnetic field. This strongly indicates the intrinsic ferromagnetic nature of Pt nanoparticles. Based on the magnetization data at 5 K, a magnetic moment of $\sim 10^{-4}\mu_B$/Pt atom could be estimated assuming that all

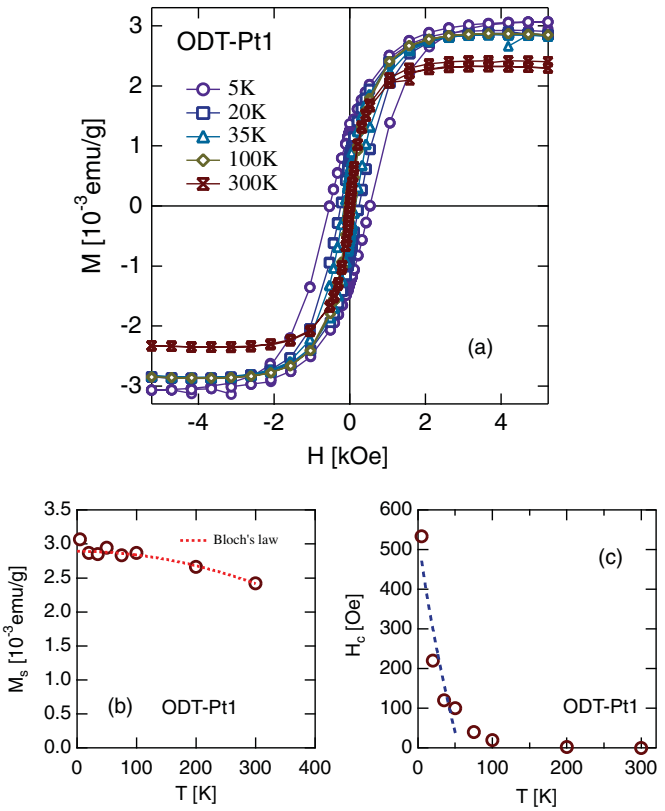

FIG. 4. (Color online) Magnetization curves of ODT-Pt1 at various temperatures are shown in (a). The spontaneous magnetization, deduced from the extrapolation of high-field data to zero magnetic field, is shown as a function of temperature. The dotted curve shows the Bloch's law fitting using $\alpha = 2$ (b). The temperature-dependent coercive force indicates a blocking temperature of ~100 K (c).

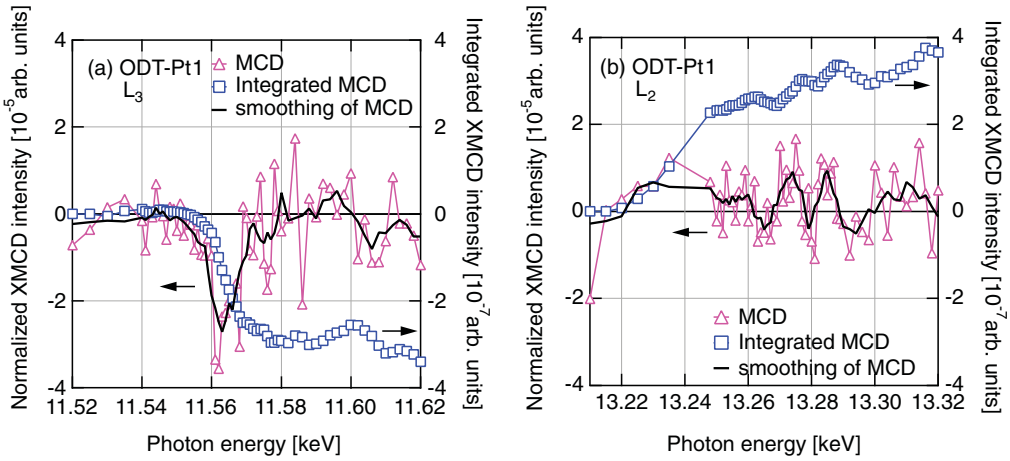

FIG. 5. (Color online) XMCD spectra and the integrated MCD intensity around L_3 (a) and L_2 (b) edges of Pt. A clear MCD peak is observed only around the L_3 edge.

the Pt atoms participated in the magnetization, and neglecting the added weight of the coating molecules. This is consistent with the magnetic moment of the Pt nanoparticle prepared by the laser ablation technique ($0.0004\mu_B$/Pt atom).[8] The spontaneous magnetization M_s, deduced by the extrapolation of the high-field magnetization data to a zero magnetic field, is plotted as a function of temperature in Fig. 4(b). This indicates that the Curie temperature of ODT-Pt1 is higher than 300 K. In addition, the temperature-dependent change above 20 K was fitted with the following expression:

$$M_s(T) = M_s(0)(1 - BT^{\alpha}), \tag{1}$$

using $M_s(0) = (2.89 \pm 0.03) \times 10^{-3}$ emu/g, $\alpha = 2.0 \pm 0.6$, and $B = (1.8 \mp 0.1) \times 10^{-6}\mathrm{K}^{-\alpha}$, where the exponent α deviates from 3/2 in the normal Bloch law for ferromagnets [solid curve in Fig. 4(b)], although the error of α is quite large. A similar deviation of α has been reported also in the other ferromagnetic particles with a nanoscale size, which led to the decrease in Curie temperature as compared with the bulk system.[32] Furthermore, we can indicate that M_s shows an upward deviation from Eq. (1) at the lowest temperature in the present measurement, although the dispersion of data is large. This kind of deviation from the Bloch-type law was explained in terms of the quantization of the spin-wave spectrum for ferrite nanoparticles.[33]

Figure 4(c) shows that the coercive force H_c of ODT-Pt1 monotonically decreases with increasing temperature and is hardly observed at temperatures above 100 K. To evaluate the anisotropy constant K_u, the low-temperature values of the coercive force are fitted by the following expression, which assumes the random orientation of the easy axis of magnetization and the negligibility of interparticle interaction:[34]

$$H_c = H_0\left\{0.479 - 0.81\left[\frac{k_B T}{2K_u v}(\ln \tau_m + 20.7)\right]^{3/4}\right\}, \tag{2}$$

where v is the volume of the nanoparticle and τ_m is the characteristic measurement time of the experiment ($\sim$100 s for static magnetic measurement). We obtained $K_u \sim 8 \times 10^7$ erg/cm^3 using $v = 3.6$ nm^3, which was evaluated based on the TEM observation. This corresponds to the blocking temperature $T_B \sim 80$ K, which is consistent with the disappearance of coercive force above 100 K.[35] The estimated value of K_u is comparable to that of the $L1_0$-type alloy FePt.[36]

XMCD measurements of ODT-Pt1 were performed to verify the intrinsic ferromagnetic contribution from Pt. Figures 5(a) and 5(b) show the XMCD spectra and the integrated MCD intensity around the L_3 and L_2 edges of Pt.[37] The XMCD peak was observed at a photon energy around the L_3 edge, above which the finite integrated intensity of the MCD signal appeared. Thus, the ferromagnetism originated from the Pt. On the other hand, there was no clear peak of MCD around the L_2 edge, and the integrated intensity gradually changed with the photon energy. No XMCD signal was reportedly detected around the L_2 edge in bulk Pt, when the magnetic moment was induced by a high magnetic field of 7 T.[38] This may indicate the pronounced contribution of orbital magnetic moment m_L in the Pt nanoparticle according to the XMCD sum rules,[39] although the signal-to-noise ratio was insufficient to qualitatively evaluate m_L. When the XMCD intensity at the L_2 edge completely disappeared, the ratio of orbital and spin magnetic moments m_L/m_S was 2/3, assuming that the contribution of the magnetic spin dipole moment was negligible.

The L_3 edge XANES spectra of ODT-Pt1 and bulk Pt are compared with that of bulk Au in Fig. 6(a), where the Pt and Au spectra are aligned in energy on the fine structure, and normalized in intensity before the edge and at the first two features after the white line. The normalized intensity obtained by subtracting the XANES spectrum of Au from that of Pt nanoparticles is shown in Fig. 6(b) to clarify the region of the white line which is associated with the dipole transition from $2p_{3/2}$ to $5d_{3/2}$ and $5d_{5/2}$, because the structures of spectra at higher energies after the white line, which are caused by the other $2p \rightarrow nd,s$ transitions, are similar for Pt and Au.[38] The integrated intensities of the white line are shown in Fig. 6(c), and the ratio of those of ODT-Pt1 and Pt bulk is shown in Fig. 6(d). The L_3 edge white line gives information about the density of the unoccupied d state.[40] The integrated intensity of ODT-Pt1 is higher than that of

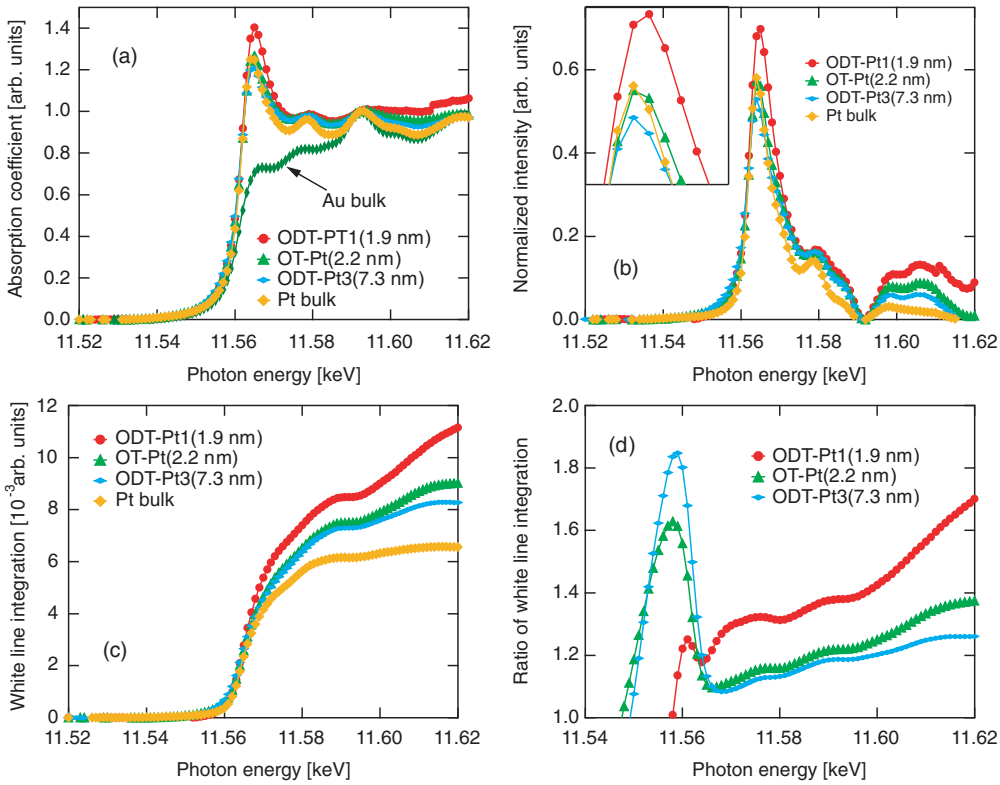

FIG. 6. (Color online) Pt L_3 edge XANES spectra of ODT-Pt1, OT-Pt, ODT-Pt3, Pt bulk, and Au bulk are shown in (a), where the Pt and Au spectra are aligned in energy on the fine structure, and normalized in intensity before the edge and at the first two features after the white line. The normalized intensity obtained by subtracting the XANES spectrum of Au from that of Pt nanoparticles is shown in (b). The integrated intensities of the white line are shown in (c), and the ratio of those for Pt nanoparticles and Pt bulk is shown in (d).

bulk Pt in Figs. 6(c) and 6(d), indicating that the number of $5d$ holes increase in Pt nanoparticles relative to the bulk sample under the plausible assumption that the transition probability is scarcely different between two samples. The slight shift of the white line of ODT-Pt1 into the high-energy side shown in the inset of Fig. 6(b) is brought about by the difference of the effective charge and interatomic distance.[41,42]

B. Magnetic behavior of Pt nanoparticles coated with alkanethiols of different carbon-chain lengths

In OT-Pt, DT-Pt, and ODT-Pt samples, Pt nanoparticles, with intrinsically the same particle size of 2 nm, are coated with alkanethiols having carbon numbers of 8, 12, and 18, respectively. Figure 7 shows the magnetic-field-dependent magnetization of OT-Pt, DT-Pt, and ODT-Pt1 samples at 5 K, where the magnetization of the nanoparticle is obtained without considering the weight of alkenethiol molecules, and this brings the error of ∼15% in magnetization.[43] All the samples show hysteresis behavior, indicating their ferromagnetic nature. The spontaneous magnetization becomes large in order DT-Pt, OT-Pt, and ODT-Pt1, even though the evaluation of magnetization includes some ambiguity. The value of H_c increased linearly with the carbon number of the alkanethiol, as shown in the inset of Fig. 7. These obviously indicate the change in magnetization and magnetic anisotropy depending on the carbon number of the coating molecules.

Figures 6(a)–6(d) show the Pt L_3 edge XANES spectra for OT-Pt and ODT-Pt1 with the carbon numbers of 8 and 18, the intensities normalized by subtracting the XANES spectrum of Au from that of the Pt nanoparticles, the integrated intensities of the white line, and the ratio of those in the Pt nanoparticle and Pt bulk, respectively. The white-line intensity of ODT-Pt1 is larger than that of OT-Pt, as shown in Fig. 6(d). This indicates that the $5d$ hole number in Pt depends on the carbon number of the alkanethiol with which the nanoparticle sample is coated, and thus the electron transfer from Pt to alkanethiol is dependent on the carbon number because the size and the surrounding circumstances of the Pt nanoparticle are intrinsically the same, so that the electronic structure of Pt is hardly affected by the differences in the alkanethiols. This indicates that the carbon number dependence of magnetization and magnetic anisotropy is correlated with the charge transfer between the Pt nanoparticle and the alkanethiol.

As shown in Fig. 8, the ESR spectra measured at room temperature reflect the carbon number dependence of magnetic anisotropy through the linewidth. The g factor and the effective linewidth ΔH, determined by the maximum and minimum in the first derivative of the ESR intensity, depend on the carbon number in a similar way (Fig. 9). Thus, the change in magnetic anisotropy, which is reflected in ΔH, correlates with the g factor, which reflects the contribution of the orbital angular momentum. Based on the g factor, the ratio of orbital and spin magnetic moments m_L/m_S of 0.094, 0.096, and 0.120 were estimated

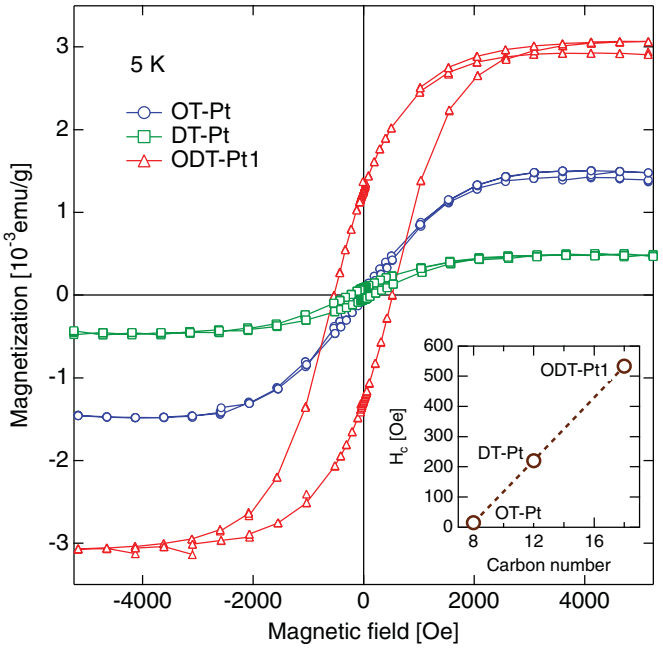

FIG. 7. (Color online) Hysteresis curves of OT-Pt, DT-Pt, and ODT-Pt1 at 5 K. The inset shows the coercive force plotted against the carbon number of the coating alkanethiol.

for carbon numbers of 8, 12, and 18, respectively, where the value of m_L/m_S is obtained as $(2-g)/2$.[44] In Table II, the ΔH, g factor, and the m_L/m_s values of the OT-Pt, DT-Pt, and ODT-Pt samples are summarized in relation with the coercive force. As discussed in Sec. IV, these correlations

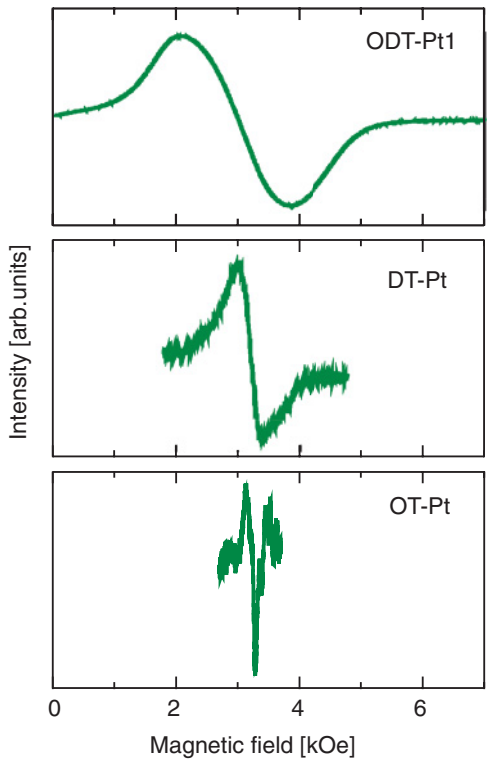

FIG. 8. (Color online) ESR spectra of ODT-Pt1, DT-Pt, and OT-Pt measured at room temperature.

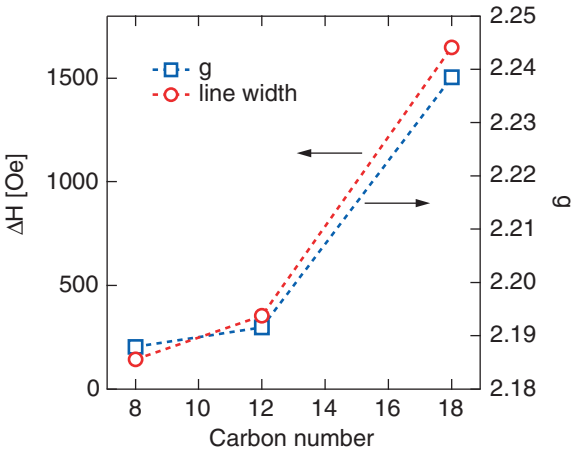

FIG. 9. (Color online) Values of the g factor and linewidth ΔH are shown against the carbon number of coating alkanethiol, and show a similar behavior.

of magnetization and magnetic anisotropy with the carbon number mainly appear through a change in the adsorption condition of alkanethiol on the Pt nanoparticle, depending on the carbon number.

C. Magnetic behavior of alkanethiol-coated Pt nanoparticles of different particle sizes

Figure 10 shows the magnetization curves at 5 K of the 1-octadecanethiol-coated Pt nanoparticles with diameters of 1.9, 5.6, and 7.3 nm, i.e., ODT-Pt1, ODT-Pt2, and ODT-Pt3. All the samples are ferromagnetic, and the spontaneous magnetization of ODT-Pt1 (diameter of 1.9 nm) is larger as compared with the other samples with a larger diameter, although there is the difference between ODT-Pt2 and ODT-Pt3 within an experimental error range. In addition, the coercive force decreases with increasing diameter, as shown in the inset. In the present nanoparticle samples the coercive force should be intrinsically attributed to magnetic anisotropy because the magnetic interaction between Pt nanoparticles is sufficiently small due to the small magnetic moment. This is also reflected in the linewidth of the ESR signal, as shown in Fig. 11, where the extra sharp signal observed for ODT-Pt2 and ODT-Pt3 can be attributed to the remaining reactive precursor or by-product in preparation method II. In addition, the diameter dependence of the g factor is similar to that of H_c (Fig. 12). Thus, the change in magnetic anisotropy originates from the contribution of the orbital angular momentum. Based on the g factor, m_L/m_S ratios of 0.120, 0.076, and 0.070

TABLE II. Coercive force, linewidth ΔH, g factor, and m_L/m_s of the prepared samples.

Sample	Coercive force (Oe)	Linewidth ΔH (Oe)	g factor	m_L/m_s
OT-Pt	15	150	2.187	0.094
DT-Pt	220	400	2.187	0.096
ODT-Pt1	530	1800	2.239	0.120
ODT-Pt2	110	440	2.151	0.076
ODT-Pt3	50	~240	2.140	0.070

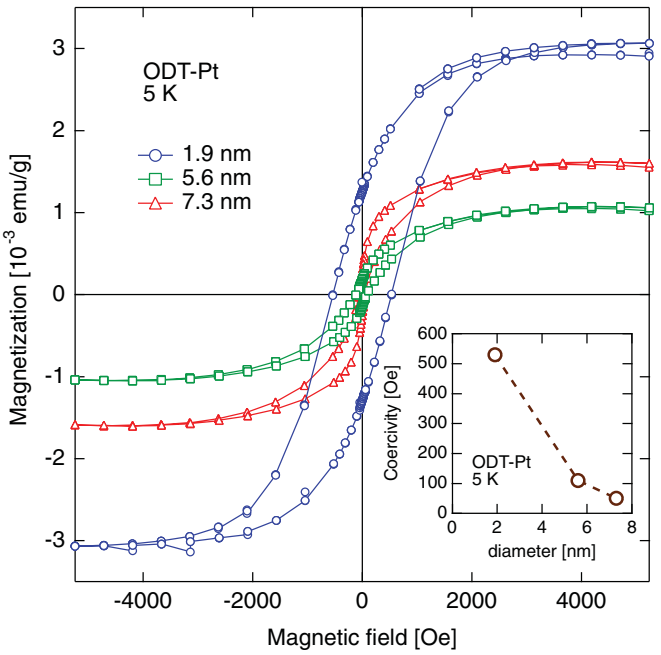

FIG. 10. (Color online) Hysteresis curves of 1-octadecanthiol-coated Pt nanoparticles with diameters of 1.9, 5.6, and 7.3 nm. The inset shows the coercive force as a function of diameter.

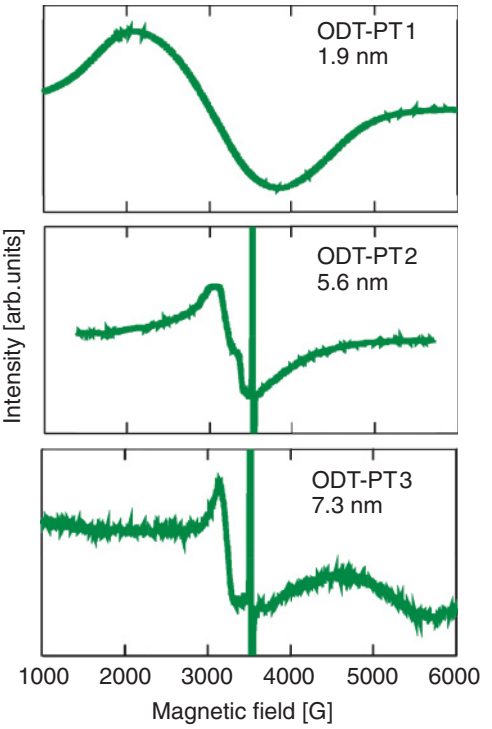

FIG. 11. (Color online) ESR spectra of ODT-Pt1 ($d = 1.9$ nm), ODT-Pt2 ($d = 5.6$ nm), and ODT-Pt3 ($d = 7.3$ nm) measured at room temperature. The extra sharp signal is attributed to the remaining reactive precursor a by-product in the preparation process.

were estimated for the particles with diameters of 1.9, 5.6, and 7.3 nm, respectively. In Table II, the ΔH, g factor and the m_L/m_s values of ODT-Pt1, ODT-Pt2, and ODT-Pt3 are summarized in relation to the coercive force.

In the XANES spectra of ODT-Pt1 and ODT-Pt3, the white-line intensity for 7.3-nm-diam particles is weaker than that for 1.9-nm-diam particles, as shown in Figs. 6(c) and 6(d). The results indicate that the hole number decreases as the size of the Pt nanoparticle increases. This should be attributed to the change in electronic structure and/or the coverage ratio of alkanethiol on the surface of the Pt nanoparticle because both ODT-Pt1 and ODT-Pt3 are coated by a common alkanethiol molecule. As discussed in Sec. IV, the particle size dependences of magnetization and magnetic anisotropy are intrinsically induced by the change in the coverage ratio of alkanethiol on the surface of the Pt nanoparticle that determines the 5d hole number. In addition, the difference in anisotropy between the surface and core region of the Pt nanoparticle must be considered.

D. Magnetic behavior of AZO-coated Pt nanoparticles with a different particle size

The magnetic-field-dependent magnetizations of AZO-Pt1 and AZO-Pt2 were obtained at 5 K before and after illumination by UV light (Fig. 13). As mentioned in Sec. II, UV illumination induces the photoisomerization of AZO from *trans* to *cis* states. Thus, the magnetizations of Pt nanoparticles affected by AZO in *trans* and *cis* states can be compared in Fig. 13. The magnetization curves of AZO-Pt1 and AZO-Pt2 show saturation behavior in magnetic fields above ~2 kOe, regardless of the light illumination. Their ferromagnetic nature is similar to that of alkanethiol-coated Pt nanoparticles. In addition, the magnetization and coercive force are intrinsically independent of the light illumination in both samples. In other words, the difference of the molecular geometry in AZO is not reflected in the magnetic behavior of the Pt nanoparticles. This is important in discussing the dependence of magnetic anisotropy on the molecular chain in relation to the dipole moment of the molecule.

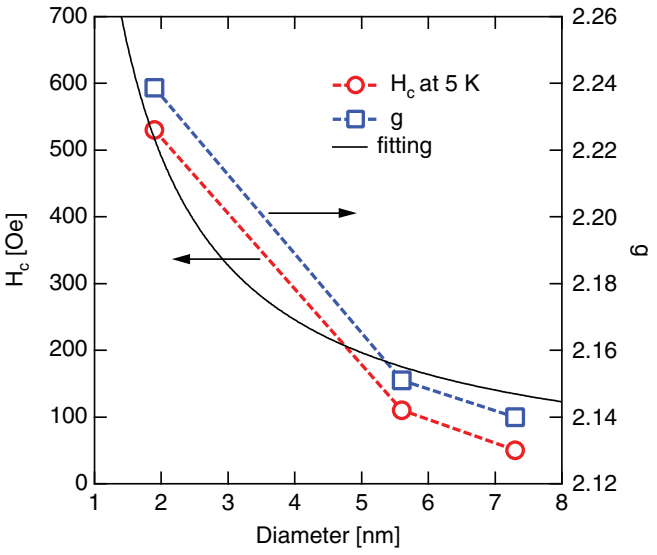

FIG. 12. (Color online) Values of the g factor and coercive force are plotted against the diameter of Pt nanoparticles. An inversely proportional relation of coercive force to diameter is roughly observed, as shown by the solid curve.

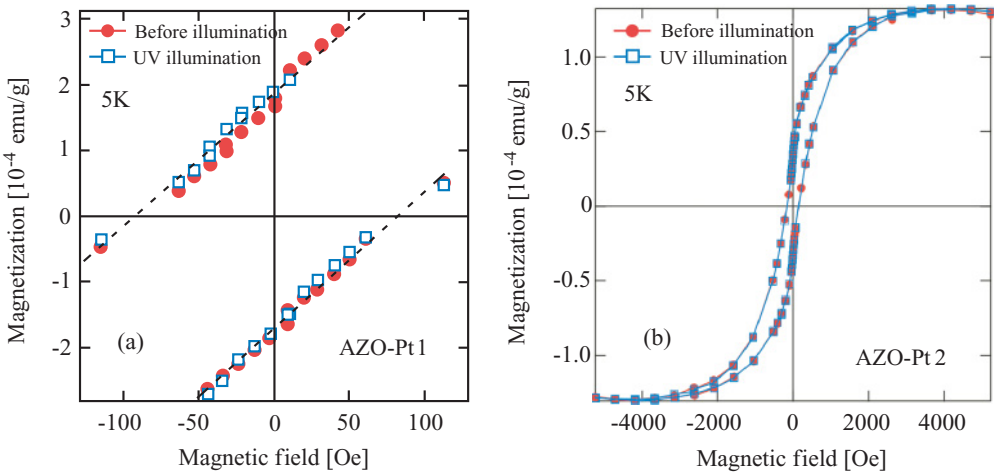

FIG. 13. (Color online) Magnetic-field-dependent magnetizations of AZO-Pt1 (a) and AZO-Pt2 (b) are obtained at 5 K before and after illumination by UV light, where the enlarged figure in the vicinity of the origin is shown for AZO-Pt1. No contribution of UV light illumination was observed in either sample.

IV. DISCUSSION

A. Mechanism for ferromagnetism appearing in Pt nanoparticles

The appearance of ferromagnetism in Pt nanoparticles coated by alkanethiol and azobenzene-derivatized thiol was confirmed even at 300 K based on the magnetic measurements, and the XMCD data showed that the magnetic polarization was inherent in Pt. Such room-temperature ferromagnetism was reported in carbon-coated Pt nanoparticles prepared by laser ablation[8] and a dodecanethiol-coated Pt branched nanostructure.[9] The ferromagnetic ordering originates from the reduced symmetry due to the twin boundary in the former system, and from the change in symmetry due to the peculiar morphology and charge transfer in the latter system. These ferromagnetic Pt systems are not identical to the present Pt nanoparticle in shape and coating material. Thus, we first discuss the origin of ferromagnetism in the present Pt nanoparticle samples based on the present XANES data, theoretical studies concerning the magnetism of Pt nanostructure,[15,16,23] and the knowledge concerning ferromagnetic Pd nanoparticles that has been accumulated thus far.[5,6,15–22]

Previous theoretical studies of Pt thin films[15,16] and nanowires[23] predicted a change in electronic structure favorable to ferromagnetism with downsizing, i.e., an increase in $D(E_F)$ which satisfies the Stoner criterion for ferromagnetism and a change in symmetry from the bulk sample. The present XANES data gives information about the 5*d* band structure and the band occupation. The change in white-line intensity in the Pt nanoparticle compared with the bulk takes place in the direction in which 5*d* holes increase, as shown in Fig. 6(d). We should note that the Fermi energy E_F in the bulk Pt is located on the high-energy side of the peak in $D(E)$.[45] Provided that this situation is maintained in the low-dimensional system of Pt, the change in white-line intensity, i.e., the increase in the 5*d* hole number, can induce ferromagnetism in nanoparticles because the $D(E_F)$ increases as the 5*d* hole number increases. In other words, the intrinsic origin of ferromagnetism in a Pt nanoparticle can be explained in terms of the change in the 5*d* hole number. On the other hand, the shift of the white line to the high-energy side suggests the change in the electron structure of the 5*d* band into the direction where the hole number decreases.[41,42] This is opposite to the expectation from the white-line intensity.

The change in the 5*d* hole number can be caused by the charge transfer between the coating molecules and the nanoparticle and/or the change in band structure that is favorable to the *s*-*d* rehybridization.[41,42] The x-ray photoelectron spectroscopy of Pt nanoparticles with diameters of 0.9–1.8 nm, coated with octadecanthiol in various coverage ratios, indicated that electrons were transferred from the nanoparticle to the coating thiol layer.[26] The charge transfer between the nanoparticle and coating molecules was explained in terms of the change in work function related to the dipole moment of the molecules.[46,47] In addition, our recent calculation of the electronic structure of (100) Pd thin films showed that the bottom of the *s* band shifted upward compared with the *d* band as the film thickness decreased,[48] leading to a decrease in the 5*d* hole number. A similar change can be recognized in Pt thin films.[49] In the present system, therefore, the size reduction of Pt should cause two changes in the opposite direction: the electron deficiency that is induced by the charge transfer from Pt to thiol and the decrease in the 5*d* hole number through the *s*-*d* rehybridization. This is consistent with the XANES data. As a result, the increase in hole number accompanied by the charge transfer from the nanoparticle to coating molecules should be intrinsic for the ferromagnetism in Pt nanoparticles under the condition that the electronic structure is weakly modified in a low-dimensional system.

When a strong modification of the electronic structure in a low-dimensional system is found, other mechanisms for ferromagnetism should be taken into account. Recently, we revealed that neutron scattering measurement of Pd nanoparticles indicated a core-shell magnetic structure.[22] Therefore, there are at least two mechanisms for ferromagnetism in nanoparticles. We showed that the standard deviation of strain

in Pd nanoparticles without a coating layer showed a positive correlation with the saturation magnetization.[21] Similar features can be expected in Pt nanoparticles. Furthermore, a recent theoretical study showed that the ferromagnetic moment appears in a specific number of layers in Pd thin films, which is triggered by quantum well states.[17] In Pt thin films as well, an oscillatory change in magnetic moment that is dependent on the number of layers was reported.[16] Based on the core-shell magnetic structure, therefore, the appearance of ferromagnetic ordering in a Pt nanoparticle can be connected with the quantum well states formed in the shell region of the particle. In addition, the ferromagnetism in the core region can be governed by strain[21] and/or the reduced symmetry due to twin formation.[8] Therefore, the change in electronic structure peculiar to low-dimensional systems, regardless of the coating molecules, should also be significant in the appearance of ferromagnetism in Pt nanoparticles.

We must comment on a previous report in which Pt nanoparticles with diameters ranging from 0.9 to 2.2 nm and coated with octadecanthiol at coverage ratios ranging from 0 to 1.05 showed no ferromagnetic behavior even at 2 K, but did show Curie-type magnetic susceptibility in addition to the temperature-independent term.[26] In the study, nanoparticles with diameter of 2.2 nm were not coated with thiol; the full coating was performed only for the smallest sample with a diameter of 0.9 nm. As compared with the present sample, this indicates that the thiol coating is intrinsic for the appearance of ferromagnetism in Pt nanoparticles, and the ferromagnetic order becomes unstable in extremely small nanoparticles, e.g., 0.9 nm in diameter, regardless of the coating. As a result, we claim that the thiol coating is indispensable for inducing ferromagnetism in Pt nanoparticles through charge transfer, although the change in the electronic structure should not be ignored.

In contrast to the conventional Stoner-type mechanism for the appearance of ferromagnetism based on electronic band picture, the origin of orbital ferromagnetism has been proposed to interpret a ferromagnetic Au nanoparticle and film with thiol coating.[43,50] A giant Lashba effect, observed in the Au film,[51] has explained the observed ferromagnetism that was accompanied by enormous magnetic anisotropy through the enhancement of the spin-orbit interaction. In this mechanism, the charge transfer associated with the adsorbed molecule induces a potential gradient at the boundary of the surface region coated with molecules, and the electron on the surface can be captured in an atomiclike orbital at the boundary. This produces the orbital momentum depending on the size of the region coated with molecules. Thus, the coverage condition of the adsorbed molecule should essentially influence the ferromagnetic behavior of nanoparticles. This can give a picture of the chain-length and particle-size-dependent magnetic behavior of the Pt nanoparticle in terms of orbital ferromagnetism. In contrast to Au, however, the spin contribution to the magnetic nature of Pt should be significant because of the unfilled character of the 5*d* band. In the present stage, it is difficult to evaluate the contribution to ferromagnetism of the Pt nanoparticle from the orbital momentum based on the new mechanism. Nevertheless, this mechanism can also play a significant role for the magnetization and magnetic anisotropy of the Pt nanoparticle.

B. Magnetization in alkanethiol-coated Pt nanoparticles dependent on the length of the molecular chain and particle size

The magnetization in alkanethiol-coated Pt nanoparticles is dependent on the length of the molecular chain and particle size. As shown in Figs. 7 and 10, ODT-Pt1, having the longest molecular chain and the smallest particle size among the prepared samples, has the largest magnetization, even though the ambiguity in the evaluation of magnetization was taken into consideration. In addition, the white-line intensity of ODT-Pt1 is larger than that in OT-Pt and ODT-Pt3 [Fig. 5(c)]. Thus, this indicates the correlation between magnetization and change in hole number in the 5*d* band through the charge transfer from adsorbed molecules. In contrast, photoisomerization of AZO between the *trans* and *cis* states barely changes the magnetization (Fig. 13). This is inconsistent with our expectation for a direct relation between magnetization and hole number, as explained below.

The electron transfer in thiol-coated metal can be affected based on two mechanisms: One is the change in work function $\Delta\Phi$ of metal dependent on the dipole moment μ of the coating molecule, and the other is the change in adsorption condition of the molecule on the surface of the nanoparticle depending on the carbon chain length. The former mechanism is based on the following expression:[46,47]

$$\Delta\Phi = \frac{\mu N \cos\theta}{\varepsilon\varepsilon_0}, \tag{3}$$

where N is the surface density of dipoles, ε_0 is the permittivity of the vacuum, ε is the dielectric constant of the coating layer, and θ is the tilt angle of the molecule with respect to the coating layer. The dipole moments of OT, DT, and ODT are calculated using WINMOSTAR[52] as 1.951, 1.959, and 1.963 D, respectively. Provided that N, θ, and ε are the same regardless of the carbon number, $\Delta\Phi$ of ODT-Pt1 is slightly larger than that of OT-Pt. This suggests that the electron transfer from the alkanethiol to the 5*d* band of Pt is enhanced in ODT-Pt1. However, such a change is too small to appear as a change in white-line intensity. Therefore, we can evaluate that the latter mechanism, i.e., change in adsorption condition of alkanethiol, is essential for the electron transfer between the coating molecules and the nanoparticle, and thus for the change in the 5*d* hole number in the present systems.

The correlation between magnetic anisotropy and the 5*d* hole number, under the condition that the electronic structure is hardly modified, can be more directly studied using change in the dipole moment of the coating molecules through the photoisomerization from *trans* to *cis* states of AZO-coated Pt nanoparticles. This is because significantly different dipole moments are expected between the two states; for example, the $\mu \cos\theta$ in the AZO-coated Au nanoparticle changes from -0.2 D for the *trans* state to 2.7 D for the *cis* state.[29] This should lead to an obvious difference of the work function in Pt nanoparticles, and thus an obvious change in the charge transfer between AZO and Pt. As shown in Fig. 13, on the other hand, the magnetization curves are intrinsically independent of the photoisomerization; i.e., the magnetization is hardly affected by the change in dipole moment between *trans* and *cis* states. This means that the magnetization is not governed by

the 5*d* band occupation, although the charge transfer should cause a change in the hole number with photoisomerization through the change in $\Delta\Phi$.

The large magnetization in ODT-Pt1, compared with OD-Pt and ODT-Pt3, should be attributed to the change in adsorption condition of alkanethiol even though the hole number changes through charge transfer. In other words, we have a plausible picture that the coverage ratio of alkanethiol on the surface of ODT-Pt1 is larger compared with OD-Pt and ODT-Pt3, and this induces the large magnetization. Previous studies, in which the adsorption condition of the self-assembled monolayer (SAM) on a metal surface was evaluated as a function of the chain length of molecules, indicated that the less ordered molecular structure was observed for a short chain length.[53,54] Thus, the SAM with a long chain length forms a more dense structure. Namely, we predict that the increase in the coverage ratio of alkanethiol on the nanoparticle surface is attributed to the enhancement of magnetization. In addition, the adsorption rate of alkanethiol was also dependent on the particle size, e.g., the coverage ratio was 1, 0.65, and 0.61 for Au particles of 12, 14, and 20 nm in diameter,[55] and 0.33 for an Au plain film,[56] respectively. This indicates that the decrease in particle size results in a high coverage ratio. Therefore, the coverage ratio of ODT-Pt1 should become large compared with ODT-Pt3 and ODT-Pt2. This also indicates the positive correlation between the coverage ratio and magnetization. Provided that the proposed mechanism for ferromagnetism of Au, as mentioned in Sec. IV A, is also effective for Pt nanoparticles, the change in coverage ratio dependent on the chain length of the coated molecule and particle size can induce the change in magnetization. This will be reconfirmed in the discussion of magnetic anisotropy in Secs. IV C and IV D.

C. Magnetic anisotropy in alkanethiol-coated Pt nanoparticles dependent on the length of the molecular chain

The magnetic anisotropy in alkanethiol-coated Pt nanoparticles significantly increases with the chain length of the alkanethiol. The enhancement of the orbital angular momentum is confirmed by the ESR measurement when the carbon number increases from 8 to 18. This should cause an increase in magnetic anisotropy through the spin-orbit interaction. Thus, the origin of the enhanced orbital angular momentum should be clarified to understand the mechanism of magnetic anisotropy dependent on the chain length of the coating molecule.

Bruno found that the orbital magnetic moment in transition-metal monolayers is governed by the crystal-field energy and the filling of the valence band using the tight-binding approach.[24] The calculated anisotropy energy of a 3*d* transition metal became enhanced with decreasing valence electrons ($3d + 4s$) from Ni, and reached a maximum around Co and then decreased. Provided that the orbital angular momentum in a Pt nanoparticle system sensitively depends on the hole number in the 5*d* band in a similar way, the change in magnetic anisotropy depending on the length of the alkanethiol chain can be understood based on the present data of white-line intensities in Figs. 6(c) and 6(d). The change in the hole number should be caused not by the modification of electronic structure, but the change in charge transfer between the coating molecules and the nanoparticle. This is because the size and surrounding circumstances of the Pt nanoparticle were essentially the same in the samples of ODT-Pt1 and OT-Pt1, indicating a small change in electronic structure depending on the carbon number.

As shown in Fig. 13, on the other hand, the magnetization curves are intrinsically independent of the photoisomerization; i.e., the magnetic anisotropy, evaluated from the coercive force, is barely affected by the change in dipole moment between *trans* and *cis* states. This means that the magnetic anisotropy is not governed by the 5*d* band occupation, which should be affected by a change in charge transfer with photoisomerization through the change in $\Delta\Phi$. Therefore, the significant enhancement of magnetic anisotropy in ODT-Pt1 compared with OD-Pt cannot be interpreted based on the previous calculation of magnetic anisotropy dependent on the band filling in the 3*d* transition metal.[24] There must be some predominant mechanisms of magnetic anisotropy other than 5*d* band occupation which are dependent on the length of the molecular chain.

Many studies have indicated the contribution of gas adsorption on the surface of 3*d* transition-metal films to magnetic anisotropy.[25,57–59] Spin orientation transition in films of Ni on Cu(001),[25,57] Fe on Cu(100),[58] and Co or Ni on Pt(111)[59] with adsorption of H_2 and/or CO, which is attributed to the change in the easy magnetization axis, has been reported. Matsumura *et al*. showed that the film thickness-dependent contribution of the orbital magnetic moment, evaluated using XMCD, caused a change in magnetic anisotropy and thus spin orientation at a critical thickness.[25] Such a change in orbital moment was dependent on the kind of gas, because the adsorption site on the surface, by which the electron rotation in an orbital is affected, is different depending on the molecule. This can explain the present dependence of magnetic moment on the length of the molecular chain.

As mentioned in Sec. IV B, the stability of alkanethiol SAM on Au(111) is increased and the more dense structure should be formed when the chain length becomes long.[53,54] The adsorption site on Au was sensitively changed under nonsaturation coverage.[60] Also in the present Pt nanoparticles, thus the coverage ratio and adsorption site can be dependent on the length of the molecular chain. As the chain length of molecules becomes long, thus the magnetic anisotropy of the Pt nanoparticle should be enhanced thorough the increase in coverage ratio. This is consistent with the picture of orbital ferromagnetism proposed for the Au nanoparticle,[43,50] in which magnetic anisotropy is governed with the orbital moment depending on the area of the domain which is uniformly coated with molecules. Such a picture is also supported by ESR measurement, which indicates an increase in the orbital angular momentum with increasing chain length. In addition, the adsorption site of alkanechiol on the Pt nanoparticle can be also related to the magnetic anisotropy, although we cannot obtain any clear evidence for it. In this context, the change in the 5*d* hole number, which depends on the amount of the charge transfer decided depending on the adsorption rate of alkanethiol, should be secondary for the magnetic anisotropy.

D. Particle size dependence of magnetic anisotropy in alkanethiol-coated Pt nanoparticles

The particle size dependence of magnetic anisotropy should be explained by taking into account two viewpoints:

(1) the enhancement of the orbital angular momentum with decreasing particle size as evaluated from the ESR data, and (2) the change in the ratio of the surface and volume dependent on the nanoparticle size. First, the discussion is performed from viewpoint (1).

As discussed in Sec. IV B, the change in orbital magnetic moment can depend on the 5*d* hole number[24] and the adsorption condition of alkanethiol on the surface of the Pt nanoparticle.[25,57–59] The change in the 5*d* hole number is attributed to the *s*-*d* rehybridization and/or charge transfer. The modification of the electronic structure of Pt, caused by downsizing, may lead to the upward shift of the *s* band compared with the *d* band to decrease the hole number, as found in Pt thin films.[49] This is inconsistent with the size dependence of the integrated white-line intensity in Fig. 6(d). The charge transfer between alkanethiol and Pt works in the direction of the increase in the 5*d* hole number. As mentioned in Sec. IV B, the stability of alkanethiol on the surface of the Au nanoparticle is significantly dependent on the curvature of the particle, i.e., the coverage ratio decreases with increasing particle size[55] and reaches the lower value for the Au plain film as compared with the particle.[56] This indicates that the decrease in particle size results in an increase in the 5*d* hole number through enhanced charge transfer. Therefore, the coverage ratio and thus the 5*d* hole number should become large in the order of ODT-Pt3, ODT-Pt2, and ODT-Pt1. This is consistent with the integrated white-line intensity. If we recall the discussion concerning the carbon chain length dependence of magnetic anisotropy, however, we cannot conclude that the change in the hole number is the intrinsic origin of the particle-size-dependent magnetic anisotropy.

The adsorption site of alkanethiol is sensitive to the coverage ratio.[56,60] Provided that the increase in coverage ratio, corresponding to the decrease in particle size, induces the surface structure of alkanethiol that is favorable to the orbital magnetic moment, the magnetic anisotropy should increase in the small nanoparticle. Such a change in surface structure is plausible, as shown in the interpretation of magnetic anisotropy dependent on the molecular chain length based on the picture of orbital ferromagnetism in the Au nanoparticle.[43,50] Therefore, the downsizing of nanoparticles can induce the enhanced contribution of the orbital angular momentum to increase the magnetic anisotropy.

In addition, the surface-to-volume ratio that is dependent on the particle size [viewpoint (2)] should be noted to discuss whether or not the magnetic anisotropy is mainly localized at the surface region. Assuming a simple core shell model in which only the shell region has magnetic anisotropy, the anisotropy energy per volume is inversely proportional to the diameter of the nanoparticle. As shown by the solid curve in Fig. 12, the coercive force roughly depends on the diameter according to such a relation. Therefore, the surface region of the Pt nanoparticle mainly connects to the magnetic anisotropy. This strongly supports the mechanism for the appearance of magnetic anisotropy through the orbital angular momentum localized on the particle surface. Namely, the mechanism of magnetic anisotropy proposed for Au nanoparticles with thiol coating should also work on that of the Pt nanoparticle.

V. CONCLUSIONS

Thiol-coated Pt nanoparticles showed ferromagnetism above room temperature, and the coercive force was sensitively dependent on the molecular length and the particle size. XMCD measurements indicated that the ferromagnetism was inherent in the Pt. The appearance of ferromagnetism is mainly interpreted based on two mechanisms. One is based on the electronic band mechanism, i.e., the increase in the hole number in the 5*d* band through the charge transfer from coating thiol and the change in the electronic structure peculiar to the nanoparticle, with which the Stoner criterion for ferromagnetism is satisfied. The other is the orbital ferromagnetism due to electrons captured in the atomiclike orbital at the boundary of the surface region, which is coated with thiol molecules. The latter mechanism provides an explanation for the change in magnetization depending on the chain length of alkanethiol and the particle size. The magnetic anisotropy of the Pt nanoparticle increased with the increasing chain length of alkanethiol and decreasing the particle size through the enhancement of the orbital angular momentum. In addition, it occurs mainly on the surface region of the Pt nanoparticle. The chain length and particle size dependences of magnetic anisotropy are intrinsically interpreted in terms of the change in the angular momentum depending on the adsorption condition, especially the coverage ratio, of alkanethiol on the surface of the Pt nanoparticle. This is consistent with the existence of a second mechanism for ferromagnetism.

We demonstrated that the magnetization and magnetic anisotropy of Pt nanoparticles could be manipulated by altering the surface coating and particle size. The origin of these effects should be understood as based on the surface structure of molecules determined by the adsorption site and coverage ratio. A further detailed study of the mechanism for adsorption of molecules on a nanoparticle is required to theoretically anticipate and achieve a desired magnetic anisotropy through such manipulations.

ACKNOWLEDGMENTS

Part of the experiment was performed at the SPring-8 with the approval of the Japan Synchrotron Radiation Research Institute (JASRI) as a Nanotechnology Support Project of The Ministry of Education, Culture, Sports, Science, and Technology (Proposal No. 2008B1804/BL-No. 39XU). This work was supported by a Grant-in-Aid for Scientific Research Programs (No. 19310077) from the Ministry of Education, Science, Sports, and Culture of Japan.

[1] S. Sun, C. B. Murray, D. Weller, L. Folks, and A. Moser, Science **287**, 1989 (2000).

[2] Y. Nishihata, J. Mizuki, T. Akao, H. Tanaka, M. Uenishi, M. Kimura, T. Okamoto, and N. Hamada, Nature (London) **418**, 164 (2002).

[3]J. J. Urban, D. V. Talapin, E. V. Shevchenko, C. R. Kagan, and C. B. Murray, Nat. Mater. **6**, 115 (2007).
[4]K. Koga, T. Ikeshoji, and K. I. Sugawara, Phys. Rev. Lett. **92**, 115507 (2004).
[5]T. Shinohara, T. Sato, and T. Taniyama, Phys. Rev. Lett. **91**, 197201 (2003); T. Taniyama, E. Ohta, and T. Sato, Europhys. Lett. **38**, 195 (1997).
[6]B. Sampedro, P. Crespo, A. Hernando, R. Litrán, J. C. Sánchez López, C. López Cartes, A. Fernandez, J. Ramírez, J. González Calbet, and M. Vallet, Phys. Rev. Lett. **91**, 237203 (2003).
[7]Y. Yamamoto, T. Miura, Y. Nakae, T. Teranishi, M. Miyake, and H. Hori, Physica B **329-333**, 1183 (2003).
[8]M. A. García, M. L. Ruiz-González, G. F. de la Fuente, P. Crespo, J. M. González, J. Llopis, J. M. González-Calbet, M. Vallet-Regí, and A. Hernando, Chem. Mater. **19**, 889 (2007).
[9]H.-T. Zhang, J. Ding, and G.-M. Chow, Langmuir **24**, 375 (2008).
[10]P. Crespo, R. Litrán, T.C. Rojas, M. Multigner, J. M. de la Fuente, J. C. Sánchez-López, M. A. García, A. Hernando, S. Penadés, and A. Fernández, Phys. Rev. Lett. **93**, 087204 (2004).
[11]Y. Yamamoto, T. Miura, M. Suzuki, N. Kawamura, H. Miyagawa, T. Nakamura, K. Kobayashi, T. Teranishi, and H. Hori, Phys. Rev. Lett. **93**, 116801 (2004).
[12]V. L. Moruzzi and P. M. Marcus, Phys. Rev. B **39**, 471 (1989).
[13]H. Chen, N. E. Brener, and J. Callaway, Phys. Rev. B **40**, 1443 (1989).
[14]A. H. MacDonald, J. M. Daams, S. H. Vosko, and D. D. Koelling, Phys. Rev. B **23**, 6377 (1981).
[15]S. Blügel, Phys. Rev. Lett. **68** 851 (1992); Europhys. Lett. **18**, 257 (1992); Solid State Commun. **84**, 621 (1992); Phys. Rev. B **51**, 2025 (1995); J. Redinger, S. Blügel, and R. Podloucky, *ibid.* **51**, 13852 (1995).
[16]A. M. N. Niklasson, S. Mirbt, H. L. Skriver, and B. Johansson, Phys. Rev. B **56**, 3276 (1997).
[17]Soon Cheol Hong, Jae Il Lee, and Ruqian Wu, Phys. Rev. B **75**, 172402 (2007).
[18]A. Delin, E. Tosatti, and R. Weht, Phys. Rev. Lett. **92**, 057201 (2004).
[19]S. S. Alexandre, E. Anglada, J. M. Soler, and F. Yndurain, Phys. Rev. B **74**, 054405 (2006).
[20]Y. Oba, H. Okamoto, T. Sato, T. Shinohara, J. Suzuki, T. Nakamura, T. Muro, and H. Osawa, J. Phys. D **41**, 134024 (2008).
[21]Yojiro Oba, Tetsuya Sato, and Takenao Shinohara, Phys. Rev. B **78**, 224417 (2008).
[22]Yojiro Oba, Takenao Shinohara, Takayuki Oku, Jun-ichi Suzuki, Masato Ohnuma, and Tetsuya Sato, J. Phys. Soc. Jpn. **78**, 044711 (2009).
[23]A. Delin and E. Tosatti, Phys. Rev. B **68**, 144434 (2003); Surf. Sci. **566-568**, 262 (2004); A. Smogunov, A. Dal Corso, A. Delin, R. Weht, and E. Tosatti, Nat. Nanotechnol. **3**, 22 (2008); Alexander Smogunov, Andrea Dal Corso, and Erio Tosatti, Phys. Rev. B **78**, 014423 (2008).
[24]Patrick Bruno, Phys. Rev. B **39**, 865 (1989).
[25]Daiju Matsumura, Toshihiko Yokoyama, Kenta Amemiya, Soichiro Kitagawa, and Toshiaki Ohta, Phys. Rev. B **66**, 024402 (2002).
[26]Weixia Tu, Kazuyuki Takai, Ken-ichi Fukui, Akira Miyazaki, and Toshiaki Enoki, J. Phys. Chem. B **107**, 10134 (2003).
[27]C. B. Murray, D. J. Norris, and M. G. Bawendi, J. Am. Chem. Soc. **115**, 8706 (1993).
[28]Jian Zhang, James K. Whitesell, and Marye Anne Fox, Chem. Mater. **13**, 1323 (2001).
[29]Masayuki Suda, Naoto Kameyama, Motohiro Suzuki, Naomi Kawamura, and Yasuaki Einaga, Angew. Chem. Int. Ed. **47**, 160 (2008).
[30]H. Maruyama, M. Suzuki, N. Kawamura, M. Ito, E. Arakawa, J. Kokubun, K. Hirano, K. Horie, S. Uemura, K. Hagiwara, M. Mizumaki, S. Goto, H. Kitamura, K. Namikawa, and T. Ishikawa, J. Synchrotron Radiat. **6**, 1133 (1999).
[31]K. Hirano, T. Ishikawa, S. Koreeda, K. Fuchigami, K. Kanzaki, and S. Kikuta, Jpn. J. Appl. Phys., Part 2 **31**, L1209 (1992).
[32]P. V. Hendriksen, S. Linderoth, and P.-A. Lindgård, J. Magn. Magn. Mater. **104-107**, 1577 (1992); Phys. Rev. B **48**, 7259 (1993).
[33]K. Mandal, Subarna Mitra, and P. Anil Kumar, Europhys. Lett. **75**, 618 (2006).
[34]J. Garcia-Otero, A. J. Garcia-Bastida, and J. Rivas, J. Magn. Magn. Mater. **189**, 377 (1998).
[35]H. Mamiya, I. Nakatani, T. Furubayashi, and M. Ohnuma, Trans. Magn. Soc. Jpn. **2**, 36 (2002).
[36]For example, Dieter Weller, Andreas Moser, Liesl Folks, Margaret E. Best, Wen Lee, Mike F. Toney, M. Schwickert, Jan-Ulrich Thiele, and Mary F. Doerner, IEEE Trans. Mag. **36**, 10 (2000).
[37]The L_3 and L_2 absorption coefficients of Pt involve an electron transition from the $2p_{3/2}(L_3)$ and $2p_{1/2}(L_2)$ core level toward the $5d$ and $6s$ unoccupied conduction states. The contribution of the d-symmetry portion is dominant and the transition from $2p$ to $6s$ is essentially negligible, because the s-symmetry portion of the density of state is small and spreads out in energy, as shown in theoretical study of white lines in x-ray absorption in M. Brown, R. E. Peierls, and E. A. Stern, Phys. Rev. B **15**, 738 (1977). This situation is intrinsically the same even in the nanoparticle system [e.g., J. Bartolomé, F. Bartolome, L. M. Garcia, E. Roduner, Y. Akdogan, F. Wilhelm, and A. Rogalev, Phys. Rev. B **80**, 014404 (2009)].
[38]J.-P. Kappler, Ph. Phresser, H. Hori, N. Jaouen, F. Wilhelm, and A. Rogalev (private communication).
[39]B. T. Thole, P. Carra, F. Sette, and G. van der Laan, Phys. Rev. Lett. **68**, 1943 (1992); P. Carra, B. T. Thole, M. Altarelli, and X. Wang, *ibid.* **70**, 694 (1993).
[40]P. Zhang and T. K. Sham, Appl. Phys. Lett. **81**, 736 (2002).
[41]Robert E. Benfield, Didier Grandjean, Michael Fröll, Raphael Pugin, Thomas Sawitowski, and Günter Schmid, J. Phys. Chem. B **105**, 1961 (2001).
[42]S. K. Pandey and A. R. Chetal, Phys. Status Solidi B **170**, 631 (1992).
[43]José S. Garitaonandia, Maite Insausti, Eider Goikolea, Motohiro Suzuki, John D. Casgion, Naomi Kawamura, Hitoshi Ohsawa, Izaskun Gil de Muro, Kiyonori Suzuki, Fernando Plazaola, and Teofilo Rojo, Nano Lett. **8**, 661 (2008).
[44]Soshin Chikazumi, *Physics of Magnetism* (Krieger, Huntington, NY, 1978), p. 52.
[45]A. H. MacDonald, J. M. Daams, S. H. Vosko, and Dd. D. Koelling, Phys. Rev. B **23**, 6377 (1981).
[46]S. G. Ray, H. Cohen, R. Naaman, Haiying Liu, and D. H. Waldeck, J. Phys. Chem. **109**, 14064 (2005).
[47]Amsala Y. Anagaw, Robert A. Wolkow, and Gino A. DiLabio, J. Phys. Chem. **112**, 3780 (2008).
[48]Taichi Urayama, Yojiro Oba, Shin Yabuuchi, Tetsuya Sato, and Hiroyuki Kageshima, J. Phys. Soc. Jpn. (submitted).

[49]K. Yamada, H. Kageshima, and T. Sato (private communication).
[50]A. Hernando, P. Crespo, and M. A. García, Phys. Rev. Lett. **96** 057206 (2006); A. Hernando, P. Crespo, and M. A. García, E. Fernández Pinel, J. de la Venta, A. Fernández, and S. Penadés, Phys. Rev. B **74**, 052403 (2006).
[51]S. LaShell, B. A. McDougall, and E. Jensen, Phys. Rev. Lett. **77**, 3419 (1996).
[52]WINMOSTAR is the molecular calculation support system developed by Norio Senda, which can be downloaded from [http://winmostar.com/index.html].
[53]Xudong Xiao, Jun Hu, Deborah H. Charych, and Miquil Salmeron, Langmuir **12**, 235 (1996).
[54]A. Lio, H. H. Charych, and M. Salmeron, J. Phys. Chem. B **101**, 3800 (1997).
[55]J. M. Ramallo-Lopez, L. J. Giovanetti, F. G. Requejo, S. R. Isaacs, Y. S. Shon, and M. Salmeron, Phys. Rev. B **74**, 073410 (2006).
[56]C. Vericat, G.A. Benitez, D. E. Grumelli, M. E. Vela, and R. C. Salvarezza, J. Phys. Condens. Matter **20**, 184004 (2008).
[57]For example, R. Vollmer, Th. Gutjahr-Löser, J. Kirschner, S. van Dijken, and B. Poelsema, Phys. Rev. B **60** (1999) 6277; S. can Dijken, R. Vollmer, B. Poelsema, and J. Kirshner, J. Magn. Magn. Mater. **210**, 316 (2000).
[58]R. Vollmer and J. Kirschner, Phys. Rev. B **61**, 4146 (2000).
[59]O. Robach, C. Quiros, P. Steadman, K. F. Peters, E. Lundgren, J. Alvarez, H. Isern, and S. Ferrer, Phys. Rev. B **65**, 054423 (2002).
[60]C. Vericat, M. E. Vela, and R. C. Salvarezza, Phys. Chem. Chem. Phys. **7**, 3258 (2005).